Three-Dimensional Structural Analysis of the Group B Polysaccharide of *Neisseria meningitidis* 6275 by Two-Dimensional NMR: The Polysaccharide Is Suggested To Exist in Helical Conformations in Solution†

Ryohei Yamasaki*,‡,§ and Bradley Bacon§

Department of Laboratory Medicine and Center for Immunochemistry, University of California, and Veterans Administration Medical Center (113A), San Francisco, California 94121

Received April 9, 1990; Revised Manuscript Received August 9, 1990

ABSTRACT: The solution conformations of the group B polysaccharide of *Neisseria meningitidis* were analyzed by DQF-COSY and pure absorption 2D NOE NMR with three mixing times. The pyranose ring of the sialic acid residue was found to be in the $^2C_5$ conformation. The DQF-COSY analysis indicated that the orientations of H6 and H7 and of H7 and H8 are both gauche. In order to overcome the difficulties in analyzing the NOE data due to the two sets of proton overlaps, molecular modeling of α-2,8-linked sialic acid oligomers was carried out to investigate possible conformers, and theoretical NOE calculations were performed by using CORMA (complete relaxation matrix analysis). Our analysis suggests that the polysaccharide adopts helical structures for which the ϕ (defined by O6–C2–O8–C8) and ψ (C2–O8–C8–C7) angles are in the following ranges: ϕ −60 to 0°, ψ 115–175° or ϕ 90–120°, ψ 55–175°. The weak affinity of anti-B antibodies for smaller α-2,8-linked oligosaccharides may be due to the fact that such oligomers are more flexible and may not form an ordered structure as the poly(sialic acid) does.

Group B capsular polysaccharide is one of the antigenic components of *Neisseria meningitidis*. The polysaccharide is a poly(sialic acid) and its repeating unit is an α-2,8-linked sialylsialic acid (Bhattacharjee et al., 1975). *Escherichia coli* can also produce the α-2,8-linked poly(sialic acid) known as the K1 antigen. The two bacteria also produce α-2,9-linked poly(sialic acid). However, the immunochemical properties of the α-2,8-linked poly(sialic acid) are very different from those of the α-2,9-linked poly(sialic acid). The latter induces a higher titer of antibodies when injected in humans and is a successful carbohydrate vaccine (Beuvery et al., 1982; Vodopija et al., 1983). Contrary to this, the α-2,8-linked poly(sialic acid) is a poor immunogen by itself (Wyle et al., 1972).

The poor immunogenicity of the group B polysaccharide of *N. meningitidis* has been postulated to be due to its structural similarity to the human tissues; the α-2,8-linked sialylsialic acid has been known to exist in human gangliosides and brain glycopeptides (Finne et al., 1983; Sonderstrom et al., 1984). Finne et al. (1983) have found that polyclonal sera raised against the polysaccharide of *E. coli* K1 bind to a brain ganglioside, and they have shown the presence of a cross-reactive epitope between the K1 polysaccharide and the brain ganglioside. Very recently, the same group confirmed the cross-reactive nature of the polysaccharide and neonatal brain tissues from humans and rats by using an IgG monoclonal antibody (Hayrinen et al., 1989). They have also shown that the critical chain length of α-2,8-linked sialic acid oligomers for the antibody binding is 10. Jennings et al. (1985) reported that large sialic acid oligomers are necessary for the recognition of the K1 antigen by an IgM antibody through inhibition studies of the binding of horse polyclonal sera to K1 polysaccharides by α-2,8-linked oligosaccharides. These studies show that the conformations of the α-2,8-linked poly(sialic acid) are critical for epitope expression. Kabat et al. (1986) noticed that human IgM specific for the K1 and the group B polysaccharides binds to denatured DNA and suggested that the net charge of the poly(sialic acid) accounts for its binding. Thus, characterization of the conformations of the α-2,8-linked sialic acid polymer is very important in order to understand the human immune response and is essential for the development of a better vaccine against group B *N. meningitidis*.

Conformational analysis of group B or K1 capsular polysaccharides was performed by Lindon et al. (1984) and by Michon et al. (1987). Lindon et al. (1984) showed the difference in segmental motions between the α-2,8- and α-2,9-linked poly(sialic acid)s and suggested the reason for the conformational difference between the two polymers. Michon et al. (1987) studied the conformations of the K1 polysaccharide together with the α-2,8-linked sialic dimer and trimer and noted the difference between the conformation of the polymer and the oligomers. However, the overall structure of the α-2,8-linked poly(sialic acid) is not yet clear. Previously, we reported the complete assignment of the ^{1}H NMR[1] spectrum of the group B polysaccharide of *N. meningitidis* (strain 6275) by 2D NMR analysis (Yamasaki, 1988). We have performed a conformational analysis of the polymer in solution by analyzing DQF-COSY and pure absorption 2D NOE spectra together with molecular modeling and theoretical NOE calculations.

Materials and Methods

The group B polysaccharide of strain 6275 of *N. meningitidis* was prepared as previously described (Yamasaki, 1988). Antigenicity of the polymer was examined with mouse IgM monoclonal and horse polyclonal antibodies by an enzyme-linked immunoassay (Engvall & Perlmann, 1972), and the

† This work was supported by a grant from the Program for Vaccine Development of the World Health Organization. This report is No. 41 from the Center for Immunochemistry, University of California, San Francisco, CA.

* Address correspondence to this author at UCSF/VAMC 113A, 4150 Clement St., San Francisco, CA 94121.

‡ University of California, San Francisco.

§ VA Medical Center, San Francisco.

[1] Abbreviations: 2D, two dimensional; CORMA, complete relaxation matrix analysis; COSY, two-dimensional correlation spectroscopy; DQF-COSY, double quantum filtered COSY; NMR, nuclear magnetic resonance; NOE, nuclear Overhauser effect.

0006-2960/91/0430-851$02.50/0

polymer was recognized by both of the antibodies. The IgM monoclonal antibody was kindly provided by Dr. W. Zollinger (Walter Reed Research Institute, Washington, DC). The polysaccharide was lyophilized in D_2O several times prior to NMR experiments.

^1H chemical shifts are relative to the chemical shift of HOD that was calibrated relative to 3,3,3-trimethyl[2,2,3,3-$^2H_4$]-propionate (TSP) as a function of temperature. All NMR experiments were performed at 25 °C on a GE 500-MHz NMR spectrometer. The double quantum filtered COSY (DQF-COSY) spectrum (Neuhaus et al., 1985; Rance et al., 1983) was acquired in the phase-sensitive mode with time-proportional phase incrementation (TPPI) (Redfield & Kunz, 1975). The spectral width was ±1420 Hz. The 512 × 4K data points were processed with a 22.5°- and a 30°-shifted sine bell in the ω_2 and ω_1 dimensions, respectively, and were zero-filled to give 1K × 4K real data points. Pure absorption 2D NOE spectra were obtained as 512 × 2K data points with three different mixing times: 50, 100, and 200 ms (States et al., 1982). For each run, the polymer (10 mg) was dissolved in D_2O (0.4 mL), and the spectral width was ±1700 Hz. The 90° pulse width was 11 μs, and the preparation delay time was 8 s. The number of acquisitions (n) was 32, and the carrier frequency was set at the HOD resonance (4.78 ppm). The data matrix was apodized in both dimensions by a 45°-shifted sine bell function for resolution enhancement and zero-filled in both dimensions to give 1K × 2K real data points. NOE intensities were quantified with programs developed by Drs. S. Manogaran and R. Scheek at the NMR Laboratory, Department of Pharmaceutical Chemistry, University of California at San Francisco (Zhou et al., 1987). Relaxation measurements were performed on a degassed sample. The longitudinal relaxation time (T_1) was measured by the inversion–recovery method (Vold et al., 1968). The transverse relaxation time (T_2) was measured on a nonspinning sample by the Carr–Purcell–Meiboom–Gill method (Meiboom & Gill, 1958). A pulse spacing, τ, of 1 ms was used, and the intensity areas of the signals were fitted to the expression $I_n = I_0 \times \exp(-4n\tau/T_2)$.

Molecular modeling was carried out by using MIDAS (Ferrin et al., 1988) at the Computer Graphics Laboratory, University of California, San Francisco. X-ray coordinates of sialic acid methyl ester were used for the construction of the α-anomer of sialic acid (Flippen, 1973). The sialic acid anomer was used for building α-2,8-linked sialic acid oligomers, and the oligosaccharide models were analyzed. The C2–O8 distance was 1.40 Å, and the glycosidic torsion angle, C2–O8–C8, was fixed to 117° in common with that found in most oligosaccharides (Bock, 1983). Conformations of the α-2,8-linked sialic acid oligomers were expressed by the angles ϕ and ψ, where ϕ is the angle O6–C2–O8–C8 and ψ the angle C2–O8–C8–C7. The nomenclature and definition are according to the IUPAC–IUB Joint Commission on Biochemical Nomenclature (1983).

Theoretical 2D NOE experiments were performed by using CORMA (complete relaxation matrix analysis) that was developed by Drs. J. Keepers, B. Borgias, and T. James (Keepers & James, 1984; Borgias & James, 1988). For the NOE calculations, isotropic motions were assumed. A correlation time (τ_c) of 2.87 ns was calculated from the experimentally determined relaxation times of H3a (T_1 = 1.1 s and T_2 = 0.020 s) according to the equation (Woessner, 1962)

$$\tau_c = 2\omega^{-1}(3T_2/T_1)^{-1/2}$$

(ω is the Larmor frequency; the equation holds when $\omega\tau_c \gg 1$). However, the calculated cross-peak NOE intensities keep increasing, whereas the experimental cross-peak NOE intensities decrease at 200 ms due to spin diffusion. We examined the cross-peak NOE intensities calculated at different correlation times (3–10 ns; data not shown) and found that theoretical intensities behave in a manner similar to those observed experimentally for correlation times over 8 ns. We therefore used a correlation time of 8 ns, a value similar to those previously reported (Gulari et al., 1979; Lindon et al., 1984). The long experimental T_2 may be contributed by the polysaccharide population of smaller molecular weight since the magnetization due to the polysaccharide population of larger molecular weight decays faster.

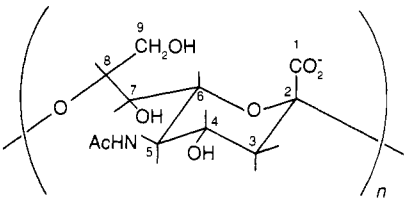

FIGURE 1: Structure of the group B polysaccharide of *N. meningitidis*.

Table I: Coupling Constants (in Hz) of the 6275 B Polymer

$J_{3a,3e}$	$J_{3a,4}$	$J_{3e,4}$	$J_{4,5}$	$J_{5,6}$	$J_{6,7}$	$J_{7,8}$	$J_{8,9}$	$J_{8,9'}$	$J_{9,9'}$
~16	~9	~5	~9	~9	<3	<3	~5	*a*	~11

[a] Could not be determined.

Results and Discussion

Since the group B polysaccharide is an α-2,8-linked poly(sialic acid) (Figure 1), its overall conformation primarily depends upon the stereochemistry of C7, C8, and O8. Previously, we reported the complete assignment of the ^1H NMR spectrum of the B polysaccharide of *N. meningitidis* of strain 6275 (Yamasaki, 1988), which was essential for analyzing 2D NOE NMR data. However, the COSY analysis of the polymer did not allow us to obtain $J_{7,8}$, $J_{8,9}$, and $J_{8,9'}$. We performed a DQF-COSY experiment to determine these coupling constants and to obtain accurate coupling constants for the rest of the protons. Figure 2 shows the 1D and DQF-COSY spectra (4.5–1.5 ppm) of the polysaccharide at 25 °C, and the coupling constants determined are shown in Table I. As discussed previously, two sets of overlap are involved: H4 and H6; H8 and H9′ (Yamasaki, 1988). Coupling constants for H3a, H3e, H4, and H5 were obtained by examination of the cross-peaks due to H3a and H3e, H3a and H4, and H3e and H4. The large H3a–H4 and small H3e–H4 couplings are apparent from the H3a–H3e cross-peak width along the ω_2 dimension; the antiphase cross-peak below the diagonal has a width of 25 Hz that consists of $J_{3a,3e}$ (active) and $J_{3a,4}$ (passive), and the one above the diagonal has a width of 11 Hz that consists of $J_{3a,3e}$ (active) and $J_{3e,4}$ (passive). In the latter case, the small passive coupling is hidden within the line width (7.5 Hz) of the antiphase doublet. Since $J_{3a,4}$ (active), $J_{3e,4}$ (passive), and $J_{4,5}$ (passive) are exhibited along the ω_2 dimension of the H3a–H4 cross-peak (above the diagonal), its width (24 Hz) indicates that the H4–H5 coupling is large. The two couplings, $J_{3a,4}$ and $J_{4,5}$, were determined to be ~9 Hz after further analysis of the cross section of the H3e–H4 cross-peak (Figure 3a). The small $J_{3e,4}$ (~5 Hz) is also obvious from the H3e–H4 cross-peak pattern (Figure 3a). From these $J_{3a,4}$, $J_{3e,4}$, and $J_{4,5}$ values, the sialic acid residue was found to be in the $^2C_5$ conformation.

As had been observed with the COSY spectrum (Yamasaki, 1988), the cross-peak due to H6 and H7 was not present in the DQF-COSY spectrum, which conffirmed a small H6–H7 coupling. The cross-peaks that appeared to be due to H6–H7

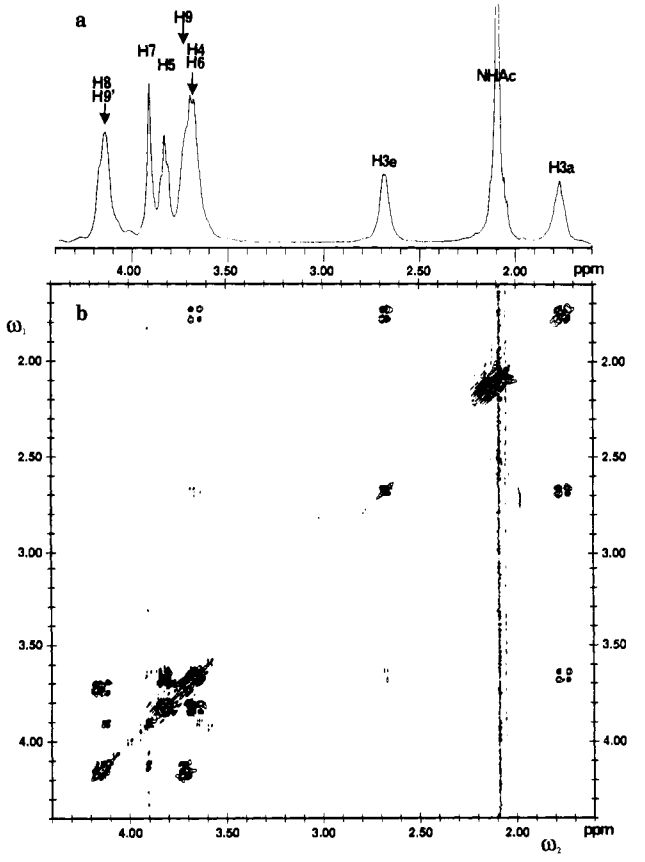

FIGURE 2: 1D (a) and DQF-COSY (b) spectra (1.5–4.5 ppm) of the B polysaccharide of strain 6275 at 25 °C. Negative levels are shaded. The digital resolution of the DQF-COSY spectrum is 0.65 Hz.

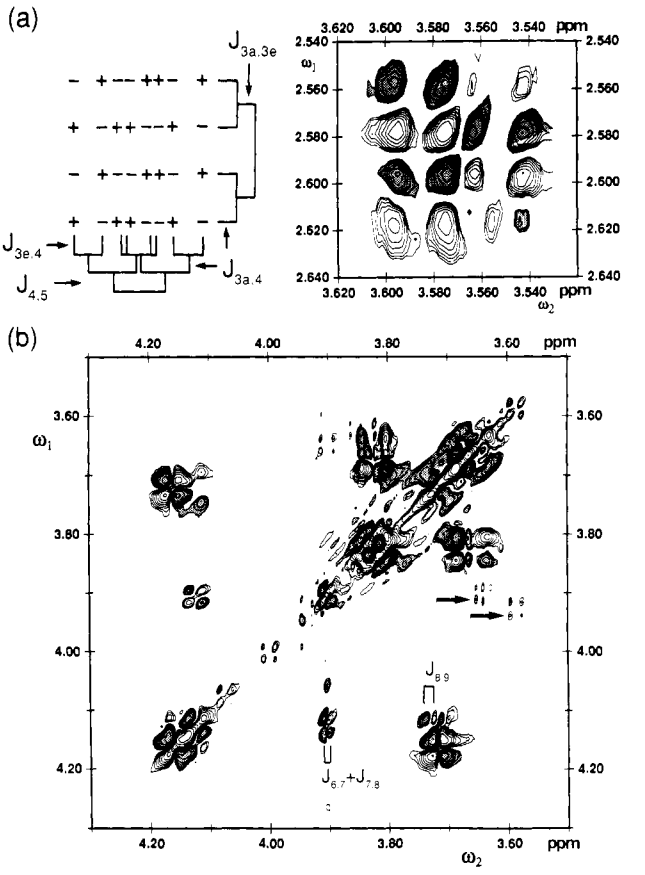

FIGURE 3: Expanded regions of the DQF-COSY spectrum from Figure 2. Negative levels are shaded. (a) The H3e–H4 cross-peak (right) and its schematic representation (left); (b) the 4.4–3.4 ppm region. The arrowed cross-peak is due to the minor populations of small sialic acid oligomers.

are actually due to protons of a minor population of sialic acid oligosaccharides (Yamasaki, 1988). The small $J_{6,7}$ coupling is supported by the cross-peak pattern (below the diagonal) of H7–H8 along the ω_2 dimension in which $J_{7,8}$ (active) and $J_{6,7}$ (passive) are exhibited. The width of the antiphase doublet (4.2 Hz; Figure 3b) shows that $J_{6,7}$ and $J_{7,8}$ are both small (<3 Hz); this indicates that both H6–H7 and H7–H8 are gauche oriented. The $J_{8,9}$ value was found to be <5 Hz from the analysis of the visible portion of the H8–H9 cross-peak, which is partially obscured by the H9–H9′ cross-peak. The ω_1 dimension of the H7–H8 cross-peak pattern (below the diagonal) suggests that $J_{8,9'}$ is small. This is also indicated by the width (12 Hz) of the H9–H9′ antiphase cross-peaks that reflect $J_{9,9'}$ (active) and $J_{8,9}$ (passive). However, we could not verify the small $J_{8,9'}$ coupling since the cross-peak pattern of the tightly coupled protons may not be first order.

Pure absorption 2D NOE experiments were performed at 25 °C with three different mixing times (50, 100, and 200 ms) (States et al., 1982), and the polymer was stable for 3 days at this temperature. Figure 4 shows a typical 2D NOE spectrum of the 6275 B polymer at 200 ms. The NOEs detected among nonvicinal protons are the following: (1) H3a and H5; (2) H3e and H5; (3) H5 and H7; (4) H5 and H8 or H9′; (5) H6 and H8 and H9′; (6) H3a and H8 or H9; (7) H3e and H8 or H9′; (8) H3a and H7; (9) H3e and H7. The $^5C_2$ conformation of the pyranose ring was supported by the detection of a stronger NOE due to H3a–H5 than to H3e–H5. The NOEs due to H5–H7 and CH_3 (NHAc)–H7 indicate that the orientation of H6 and H7 is (A) (Figure 5) rather than (B). The NOE intensity due to H5 and H7 indicates that the distance between the two protons is in the range of that between H3e and H5. As can be seen from Figure 5, conformers A and B, H5 and H7 are further apart in conformer B as are

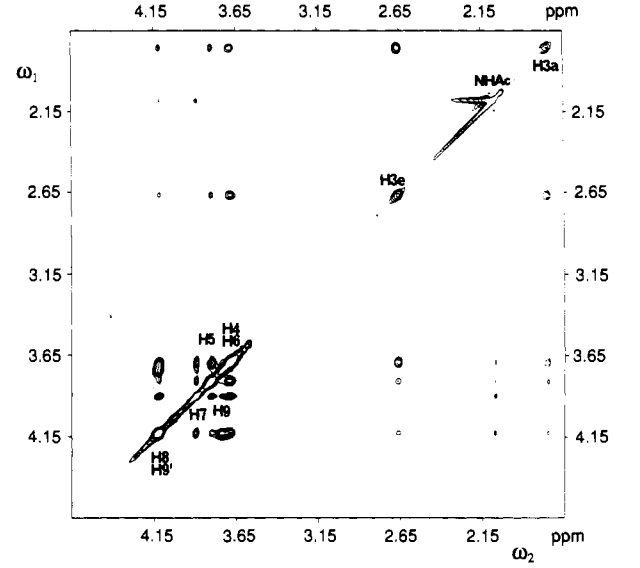

FIGURE 4: Pure absorption NOE spectrum of the 6275 B polysaccharide at 25 °C (τ_m = 200 ms).

H7 and NHAc. The detection of an NOE due to CH_3 (NHAc) and H7 also indicates that the stereochemistry of C7 is as depicted in Figure 5A. Two conformations (A and B in Figure 6) are possible with the gauche orientation of H7 and H8 if we assume only staggered conformations. Although we performed theoretical NOE calculations of conformers A and B (Figure 6) and comparative analysis of the experimental and theoretical NOE data, we could not determine the C8 stereochemistry. We were only able to exclude the C9 rotamer c

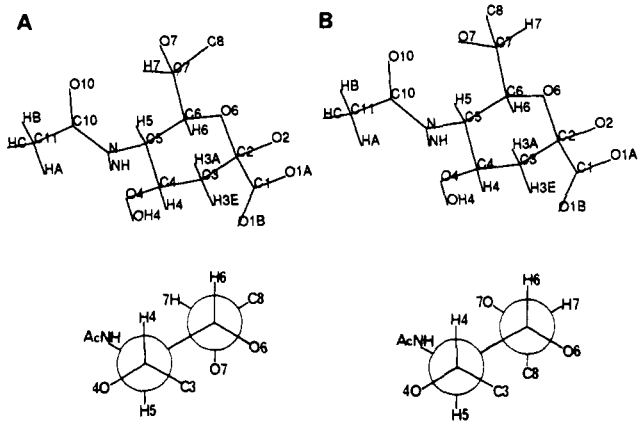

FIGURE 5: Two staggered conformers of C7 and their Newman projections, C4 → C5 (A) and C6 → C7 (B).

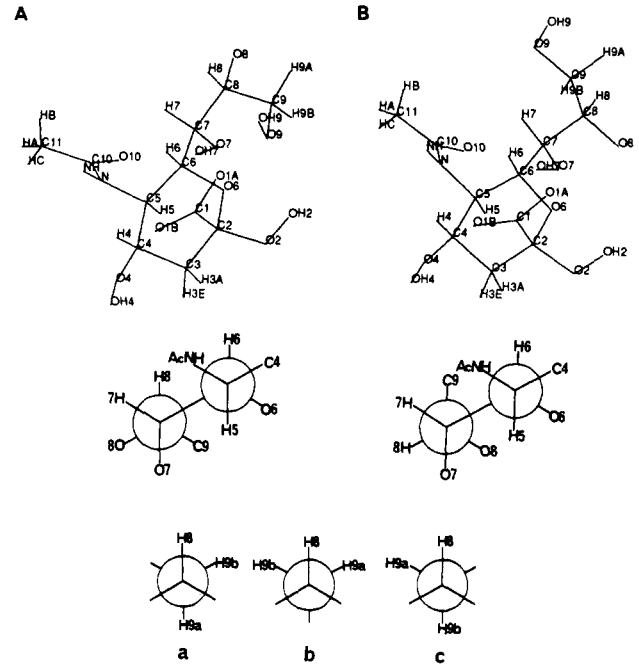

FIGURE 6: Two staggered conformers of C8 and their Newman projections, C5 → C6 (A) and C7 → C8 (B), shown together with staggered C9 rotamers a, b, and c.

(Figure 5) from having the conformer A stereochemistry due to the short O6–O9 distance (2.02 Å).

In order to solve the complications in interpreting the NOE data and in determining the overall conformations of the polymer, we performed molecular modeling and theoretical NOE calculations by using CORMA (Keepers & James, 1984; Borgias & James, 1988). Since the intraresidual distances between the C3 and the exocyclic protons are more than 5 Å, the observed NOEs among them are obviously due to interresidual proton interactions. These interresidual NOEs can be either (1) NOEs due to the C3 and exocyclic protons of adjacent residues or (2) NOEs due to the C3 and exocyclic protons of nonadjacent residues. Such identification of the interresidual NOEs is not possible by simply examining the stereochemistry of the repeating α-2,8-linked disaccharide. Therefore, we used an α-2,8-linked tetramer for modeling in order to identify intra- and interresidual NOEs and to sort out possible conformers. Then we examined the octamer model to determine possible overall conformations of the polymer; the tetramer and octamer models were constructed from the α-anomer of sialic acid by using MIDAS (Ferrin et al., 1988). The C2–O8–C8 bond angle and the C2–O8 distance were

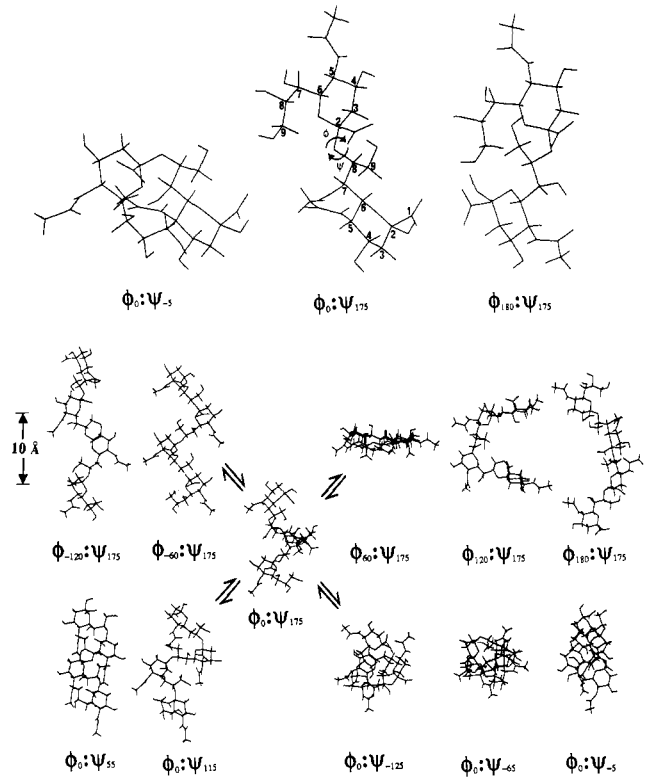

FIGURE 7: Dimer conformers having Figure 6A stereochemistry, ϕ_0:ψ_{-5}, ϕ_0:ψ_{175}, and ϕ_{180}:ψ_{175}, shown together with tetramer conformers. The ϕ angle of the ψ_{175} tetramer and the ψ angle of the ϕ_0 tetramer were rotated.

fixed at 117° (Bock, 1983) and 1.40 Å, respectively. Theoretical NOE calculations of selected models were performed, and we examined interresidual NOEs due to the C3 and exocyclic protons to determine possible conformations.

We examined the two tetramers having the A and B stereochemistry of Figure 6 by rotating each of their ϕ (defined by the C2–O8–O8–C7) and ψ (defined by the O6–C2–O8–C8) dihedral angles in 30° increments. Only two staggered rotamer populations (a and b) were considered with the tetramer having the A stereochemistry of Figure 6. Typical examples of modeling analysis are shown with tetramers having the A and B stereochemistry in Figures 7 and 8, respectively; the ϕ angle of the ψ_{175} conformer and the ψ angle of the ϕ_0 conformer were rotated with the tetramer model A, whereas the ϕ angle of the ψ_{115} conformer and the ψ angle of the ϕ_{120} conformer were rotated with the tetramer model B. Only rotamers in 60° increments are presented in the figures. Also, the analysis of interresidual distances between the C3 methylene and the exocyclic protons of the rotamers in 60° increments of two tetramer models are presented in the supplementary material.

We have found that tetramer models form helical structures regardless of the H7–H8 orientation in the range where the models can be built. The tetramer A model of Figure 6 could not be built, or was sterically overcrowded, when ψ is −125° to 85°. When ϕ is −60° to 120° and ψ is in the preceding range, a collision can occur between adjacent residues or residues that are more than one residue apart from each other (ϕ_0:$\psi_{-120-55}$ in Figure 7 are typical examples). Also, steric crowding between the adjacent and nonadjacent residues occurs in the areas where C1, C3, C5, C6, O6, and C7–C9 are involved, which can be visualized by the three dimer models in Figure 7: ϕ_0:ψ_{-5}; ϕ_0:ψ_{175}; ϕ_{180}:ψ_{175}. For the rest of the ϕ angle, the area of C3 and the exocyclic carbon of the tetramer model are extremely crowded, and the interresidual distances

Table II: Experimental NOE Intensities of the 6275 B Polymer at 25 °C with Mixing Times of 50, 100, and 200 ms and Theoretical NOEs of Selected Tetramer Models[a]

	exptl NOE		tetramer model A						tetramer model 6B			
			ϕ_{-60}:ψ_{175}		ϕ_0:ψ_{175}		ϕ_{180}:ψ_{175}		ϕ_{60}:ψ_{115}		ϕ_{120}:ψ_{115}	
	H3a	H3e	H3a	H3e	H3a	H3e	H3a	H3e	H3a	H3e	H3a	H3e
H7	5	5	3	2	1	1	5	7	5	6	1	1
	14	15	8	6	3	2	12	10	15	18	3	3
	31	33	24	20	9	8	33	32	42	44	8	8
H8, H9′	25	16	44	22	7	3	28	54	52	111	3	4
			(63)	(40)	(14)	(6)	(27)	(52)	(105)	(163)	(5)	(4)
	32	28	71	52	14	10	55	65	98	134	7	7
			(84)	(68)	(19)	(13)	(46)	(62)	(131)	(145)	(9)	(8)
	52	50	122	108	33	26	92	87	163	172	17	16
			(129)	(119)	(38)	(31)	(80)	(85)	(171)	(172)	(18)	(17)
H9	3	5	49	33	12	5	2	4	86	133	3	1
			(30)	(16)	(5)	(2)	(3)	(5)	(33)	(81)	(1)	(1)
	9	6	61	51	15	9	5	8	96	101	5	3
			(48)	(17)	(9)	(6)	(7)	(11)	(63)	(90)	(3)	(2)
	12	17	85	80	24	20	19	24	106	101	9	8
			(77)	(38)	(19)	(15)	(23)	(27)	(97)	(101)	(8)	(7)

[a] The top row represents the NOE intensities at 50 ms, the middle at 100 ms, and the bottom at 200 ms. Two calculated NOE intensities are presented for interactions involving H9 and H9′: the first reflects an arbitrary assignment of the two H9 protons from the theoretical structure to H9A and H9B; the second value (in parentheses) reverses this assignment.

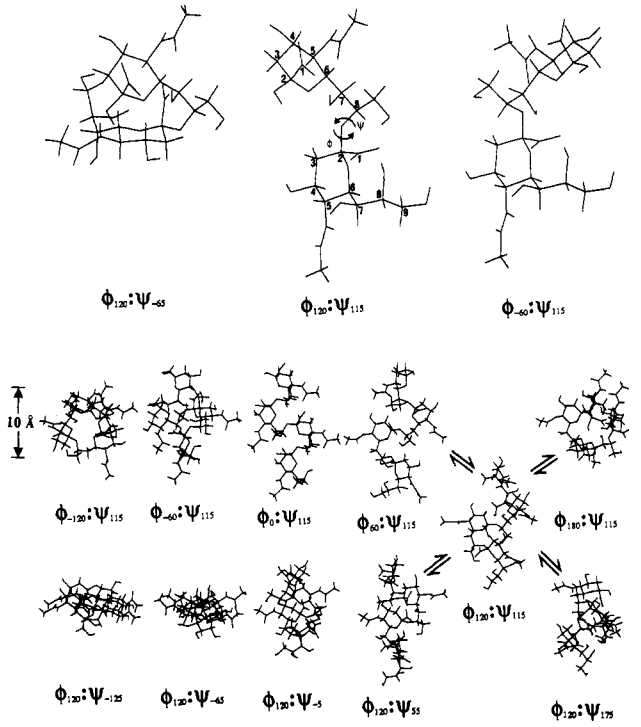

FIGURE 8: Dimer conformers having Figure 6B stereochemistry, ϕ_{120}:ψ_{-65}, ϕ_{120}:ψ_{115}, and ϕ_{-60}:ψ_{115}, shown together with tetramer conformers. The ϕ angle of the ψ_{115} tetramer and the ψ angle of the ϕ_{120} tetramer were rotated.

among the C3 and the exocyclic protons become less than the one for the van der Waals radius (1.007 Å) (Ferrin et al., 1988) for hydrogen. From this molecular modeling, the possible conformers were found to be in the ψ range of 115–175° except when the ϕ angle is around 60°. The ϕ_{180} tetramer having the A stereochemistry of Figure 6 forms a stretched helical structure (see ϕ_{180}:ψ_{175} in Figure 7) and tighter helical coils when the ϕ angle is rotated either clockwise or anticlockwise. The collision between nonadjacent residues occurs when ψ is around 60°. Since the area between the C3 and exocyclic carbons of adjacent residues are crowded when ϕ is from 180° to −60°, conformers in this ϕ range are obviously not dominant ones.

The tetramer model having the B stereochemistry of Figure 6 was found to be more sterically crowded than the one having the A stereochemistry (Figure 8). Similar to the case of the A tetramer models, collision and steric crowding between the adjacent and nonadjacent residues occur if the ψ is −155° to 55° except when ϕ is 60–120°. With this ϕ range, the ψ_{55} conformer was less sterically crowded. However, when ϕ is from 150° to −60°, severe steric crowding takes place (see the ϕ_{180}, ϕ_{-120}, and ϕ_{-60} conformers in Figure 8). Thus, possible conformers were found in the following ϕ and ψ ranges: ϕ = −30° to 120° and ψ = 55–175°.

In order to evaluate possible conformers in the selected range of ϕ and ψ angles as described above, we performed a theoretical NOE analysis of selected tetramer models. The C9 rotamer a (Figure 6) was used for the calculation since the interresidual distances between the C3 and C9 methylene protons are similar among the rotamers. The theoretical and experimental data are presented in Table II. Since some of the experimental NOE peaks were not isolated, only the interresidual NOEs due to the C3 methylene and exocyclic protons are shown, and their intensities are referenced to the H3a–H3e cross-peak intensity. With the A tetramer model of Figure 6, interresidual NOEs between the C3 and exocyclic protons were found to be between adjacent residues. The ϕ_0:ψ_{175} conformer that represents the conformers of the ψ angle of 115–175° gave interresidual NOE intensities that are comparable to those of the experimental NOEs. The larger interresidual NOEs due to the C3 methylene protons and H7 were obtained with the ϕ_{180}:ψ_{175} conformer. However, as expected from the short distances between H8 and H3a or H3e (2.68 and 2.06 Å, respectively), theoretical NOEs due to H3a and H8–H9′ were large at longer mixing times (τ_m = 100 and 200 ms). Also, the NOEs due to H3e and H8–H9′ were much larger than those due to H3a and H8–H9′ at a short mixing time (τ_m = 50 ms). Anticlockwise rotation (the decrease of the ϕ angle value) of the ϕ angle in this model reduced the intensities of the NOEs due to H3a and H8 or C9 methylene protons. However, with a ϕ angle of 90–150°, the H3e–H7 or –H8 distances became shorter. As a result, higher NOEs were detected with the exocyclic protons and H3e than those detected with the exocyclic protons and H3a, similar to the ψ_{175} conformer. Clockwise rotation of the ψ angle (ψ angle decreases) of the 90–150° ϕ range resulted in further shortening the H3e–H7 distance and did not change the above NOE pattern. Rotation of the ϕ angle of ϕ_{180}:ψ_{175} clockwise (ϕ becomes negative) resulted in shorter distances between the

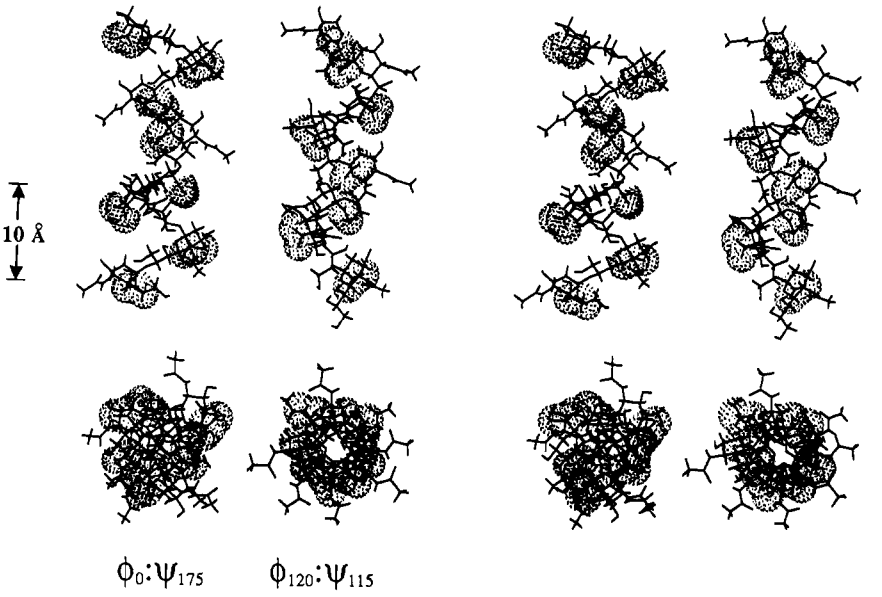

FIGURE 9: Stereo diagrams of possible octamer conformers having Figure 6A (ϕ_0:ψ_{175}) and Figure 6B (ϕ_{120}:ψ_{115}) stereochemistry. The van der Waals surfaces of the carboxyl groups are shown with the models.

C3 methylene protons and C8 or C9 protons. The interresidual NOEs became much higher than the experimental ones but the interresidual NOEs due to H3a and the exocyclic protons became higher than those due to H3e and the exocyclic ones as observed with the experimental NOEs (see the ϕ_{-60}:ψ_{175} conformer in Table II). When ϕ is between −150° and −90°, the interresidual NOE values became much higher than those of the ϕ_{-60} conformer (data not shown). These results suggest that conformers with ϕ angles of 120° to −90° are not possible and that conformers may exist with ϕ angles of −60° to 0°, the less sterically hindered conformers, such as ϕ_0, being dominant.

In contrast to the A tetramer of Figure 6, the distances of the C3 and exocyclic protons between adjacent residues of the B tetramer are more than 5 Å when ϕ is between 30° and 120°, and the interresidual NOEs were found to be due to the residues that are one residue apart. The interresidual proton distances between the nonadjacent residues became shortest when ϕ is around 60°. The shortest distance between H3e and C9 methylene protons of the ϕ_{60}:ψ_{115} was in the range of 1.4–2.0 Å regardless of the C9 stereochemistry. As a result, the NOEs due to the C3 methylene protons and H8–H9′ or H9 became much larger than the experimental ones. Also, the NOEs due to H3e and H8–H9′ or H9 were large compared with those due to H3a and H8–H9′ or H9. Rotation of the ϕ angle of this model either clockwise or anticlockwise eliminated the steric crowding. However, anticlockwise rotation of the ϕ angle (ϕ decreases) shortened the distances between H3e and H7 or H8 (for example, the H3e–H7 distance of the ϕ_0:ψ_{115} conformer was 2.67 Å), whereas clockwise rotation of the ϕ angle did not. Therefore, the possible conformers for the B tetramer are suggested to be in the narrow range of the following ϕ and ψ angles: ϕ = 90–120° and ψ = 55–175°.

Two octamer models having the A (ϕ_0:ψ_{175}) and B (ϕ_{120}:ψ_{115}) stereochemistry of Figure 6 are shown in Figure 9 as examples of possible conformers. Almost four sialic acid residues form one turn of the helix with a pitch of 10–11 Å, even though both helical coils are not symmetrical. These helical structures of the octamers are tighter than those of double-stranded DNA coils in which the pitch is around 34 Å (Dickerson et al., 1983). The pyranose rings are located almost perpendicular to each other, and the orientation of the carboxy and NHAc groups alternates, which indicates that the polymer may form tertiary structures through hydrogen bondings between chains.

It has been suggested that the carboxyl groups of the K1 polysaccharide are lined up on one side of the polymer on the basis of 1D transient NOE experiments (Michon et al., 1987). Our analysis excludes the possibility of this conformation. The analysis of 1D NOE data is ambiguous for the following reasons: (1) there are no clear explanations for the assignment of the ^{1}H NMR spectrum of the K1 polysaccharide; (2) how the proton coupling constants were determined was not given although the K1 polymer also gave a complex NMR spectrum; (3) most importantly, the identification of NOE intensities and the interpretation of NOE values of the polymer were not described.

In the present study, we were not able to determine the H7–H8 orientation of the polymer. However, from the experimental and theoretical NOE experiments combined with computer graphics modeling, we suggest that the polymer adopts helical structures in solution. The ϕ and ψ angles are in the ranges ϕ −60 to 0°, ψ 115–175° or ϕ 90–120°, ψ 55–175°, and three to four sialic acid residues form one turn of the helix with a pitch of 9–11 Å when ϕ and ψ are in the preceding ranges. This structure may not represent the structure of the intact polymer of the bacterium, although monoclonal and polyclonal antibodies recognize the polysaccharide and the bacterium. However, our findings may explain why an anti-B antibody shows weak affinity for smaller α-2,8-linked sialic acid oligomers such as the dimer or trimer (Jennings et al., 1985; Hayrinen et al., 1989) that are more flexible and may not form an ordered structure as the poly(sialic acid) does.

ACKNOWLEDGMENTS

We thank Drs. Brandan Borgias, Paul Thomas, and Tom James for their help in using the CORMA program. We also thank Drs. Vladimir Basus and Debbie Kerwood for reading the manuscript and for their editorial comments. We gratefully acknowledge the use of the UCSF Computer Graphics Laboratory (Dr. R. Langridge, Director, supported by NIH Grant RR 01081).

SUPPLEMENTARY MATERIAL AVAILABLE

Two tables of the interresidual distances between the C3 methylene and exocyclic protons of two tetramer models (4

pages). Ordering information is given on any current masthead page.

Registry No. Poly(α-2,8-sialylsialic acid), 82803-97-2.

REFERENCES

Beuvery, E. C., Leussink, A. B., Van Delft, R. W., Tiesjema, R. H., & Nagel, J. (1982) *Infect. Immun. 37*, 579–585.

Bhattacharjee, A. K., Jennings, H. J., Kenny, C. P., Martin, A., & Smith, I. C. P. (1975) *J. Biol. Chem. 250*, 1926–1932.

Bock, K. (1983) *Pure Appl. Chem. 55*, 605–622.

Borgias, B. A., & James, T. L. (1988) *J. Magn. Reson. 79*, 493–512.

Brown, E. B., Brey, W. S., Jr., & Weltner, W., Jr. (1975) *Biochim. Biophys. Acta 399*, 124–130.

Dickerson, R. E., Corner, B. N., Kopka, M. L., & Drew, H. R. (1983) in *Nucleic Acid Research* (Mizubuchi, K., Watanabe, I., & Watson, J. D., Eds.) pp 35–59, Academic Press, New York.

Engvall, E., & Perlmann, P. (1972) *J. Immunol. 109*, 129–135.

Ferrin, T. E., Huang, C. C., Jarvis, L. E., & Langridge, R. (1988) *J. Mol. Graphics 6*, 1–12.

Finne, J., Leinonen, M., & Makela, P. H. (1983) *Lancet*, 355–357.

Flippen, J. L. (1973) *Acta Crystallogr., Sect. B: Struct. Crystallogr. Cryst. Chem. 29*, 1881–1886.

Gulari, E., Chu, B., & Liu, T. Y. (1979) *Biopolymers 18*, 2943–2961.

Hayrinen, J., Bitter-Suermann, D., & Finne, J. (1989) *Mol. Immunol. 26*, 523–529.

IUPAC–IUB Joint Commission on Biochemical Nomenclature (1983) *Eur. J. Biochem. 131*, 5–7.

Jennings, H. J., Roy, R., & Michon, F. (1985) *J. Immunol. 134*, 2651–2657.

Kabat, E. A., Nickerson, K. G., Liao, J., Grossbard, L., Osserman, E. F., Glickman, E., Chess, L., Robbins, J. B., Schneerson, R., & Yang, Y. (1986) *J. Exp. Med. 164*, 642–654.

Keepers, J. W., & James, T. L. (1984) *J. Magn. Reson. 57*, 404–426.

Lindon, J. C., Vinter, J. G., Lifely, M. R., & Moreno, C. (1984) *Carbohydr. Res. 133*, 59–74.

Meiboom, S., & Gill, D. (1958) *Rev. Sci. Instrum. 29*, 688–691.

Michon, F., Brisson, J.-R., & Jennings, H. J. (1987) *Biochemistry 26*, 8399–8405.

Neuhaus, D., Wagner, G., Vasak, M., Kagi, J. H. R., & Wuthrich, K. (1985) *Eur. J. Biochem. 151*, 257–273.

Ramachandran, G. N., & Sasisekharan, V. (1968) *Adv. Protein Chem. 23*, 283–437.

Rance, M., Sorensen, O. W., Bodenhausen, G., Wagner, G., Ernst, R. R., & Wuthrich, K. (1983) *Biochem. Biophys. Res. Commun. 117*, 479–485.

Redfield, A. G., & Kunz, S. D. (1975) *J. Magn. Reson. 19*, 250–254.

Rohrer, D. C., Sarko, A., Bluhm, T. L., & Lee, Y. N. (1980) *Acta Crystallogr., Sect. B: Struct. Crystallogr. Cryst. Chem. 36*, 650–654.

Sonderstrom, T., Hansson, G., & Larson, G. (1984) *N. Engl. J. Med. 310*, 726–727.

States, D. J., Haberkorn, R. A., & Ruben, D. J. (1982) *J. Magn. Reson. 48*, 286–292.

Vodopija, I., Baklaic, Z., Hauser, P., Roelants, P., Andre, F. E., & Safary, A. (1983) *Infect. Immun. 42*, 599–604.

Vold, R. L., Waugh, J. S., Klein, M. P., & Phelps, D. E. (1968) *J. Chem. Phys. 48*, 3831–3832.

Woessner, D. E. (1962) *J. Chem. Phys. 36*, 1–4.

Wyle, F. A., Artenstein, M. S., Brandt, B. L., Tramont, E. C., Kasper, D. L., Alteri, P. L., Berman, L., & Lowenthal, P. (1972) *J. Infect. Dis. 126*, 514–522.

Yamasaki, R. (1988) *Biochem. Biophys. Res. Commun. 154*, 159–164.

Zhou, N., Bianucci A. M., Pattabiramin, N., & James, T. L. (1987) *Biochemistry 26*, 7905–7913.